

C.2 Study Site FBG2 (prostrate dwarf shrub community)

I Location

| Name | Location | Latitude | Longitude | Altitude |
|-------------|---|-----------|--------------|----------|
| FBG2 | Franklin Bluffs, Arctic North Slope, Alaska, United States of America | 69.67443° | -148.720725° | 122 m |

At an average elevation of 90 m, Franklin Bluffs is located in Subzone D about 1 km west of the Dalton Highway across from the pipeline access road APL/AMS 130 near green mile marker 375. This access road provides parking at the site. Three 10 x 10 m grids, designated dry, mesic, and wet, have been established at this location in 2002. The goniometer measurements have been carried out next to the moist / zonal site (FB_m/z). [Barreda *et al.*, 2006]

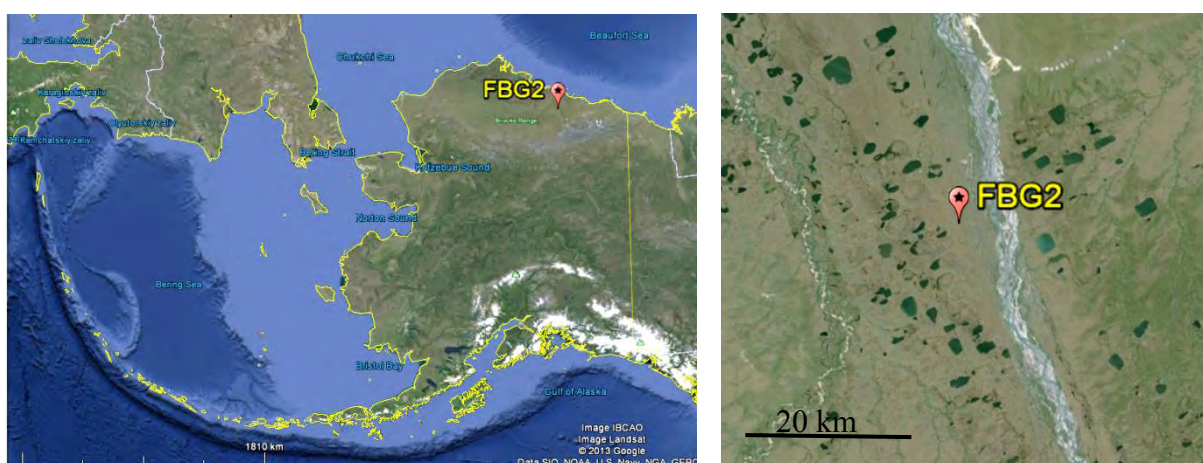


Figure C.2-1: Location of study site FBG2 in Alaska, USA. *Source:* Google Earth, 2013



Figure C.2-2: Aerial photo of a 10 x 10 m zonal grid at the Franklin Bluffs study location near the FBG2 site. *Source:* [Barreda *et al.*, 2006]

II Main Vegetation Description

The vegetation at the mesic Franklin Bluffs study location corresponds to the zonal vegetation in subzone D. The zonal plant community of bioclimate subzone D in northern Alaska is *Dryado integrifoliae-Caricetum bigelowii* [Walker et al., 2005], also called moist non-acidic tundra (MNT), or ‘nontussock sedge, dwarf-shrub, moss tundra’ [Walker et al., 2005]. It occurs on circumneutral to basic soils in association with silty loess that is blown from the major rivers in the eastern part of the Arctic Coastal Plain. The average soil pH of this plant community at Franklin Bluffs is 7.9; the average volumetric soil moisture of the top mineral horizon is 45 %, and average depth of thaw by late summer is 40 cm [Kade et al., 2005]. The dominant plants in MNT are sedges (*Carex bigelowii*, *Eriophorum angustifolium* ssp. *triste*, *C. membranacea*, *C. scirpoidea*, *E. vaginatum*), prostrate and hemi-prostrate evergreen dwarf shrubs (*Dryas integrifolia*, *Cassiope tetragona*), prostrate dwarf deciduous shrubs (*Salix arctica*, *S. reticulata*, *Arctous rubra*), scattered erect dwarf deciduous shrubs (*Salix lanata*, *S. glauca*), several forbs (*Papaver macounii*, *Pedicularis lanata*, *Saussurea angustifolia*, *Senecio atropurpureus*, *Pedicularis capitata*, *Polygonum viviparum*, *Cardamine hyperborea*, *Astragalus umbellatus*), mosses (*Tomentypnum nitens*, *Hylocomium splendens*, *Aulacomnium turgidum*, *Rhytidium rugosum*, *Hypnum bambergeri*, *Distichium capillaceum*, *Ditrichum flexicaule*), and lichens (*Thamnolia subuliformis*, *Cetraria* spp.).

An important component of the MNT is the abundant nonsorted circles, also called frost boils, which are small patterned ground features caused by soil frost heave [Walker et al., 2008; Washburn, 1980]. These features cover large parts of most MNT surfaces. The 10 x 10 m zonal grid at Franklin Bluffs has about 30 % cover of nonsorted circles. These features have drier plant communities than the mesic zonal plant communities between the circles, with high cover of lichens and bare soil.

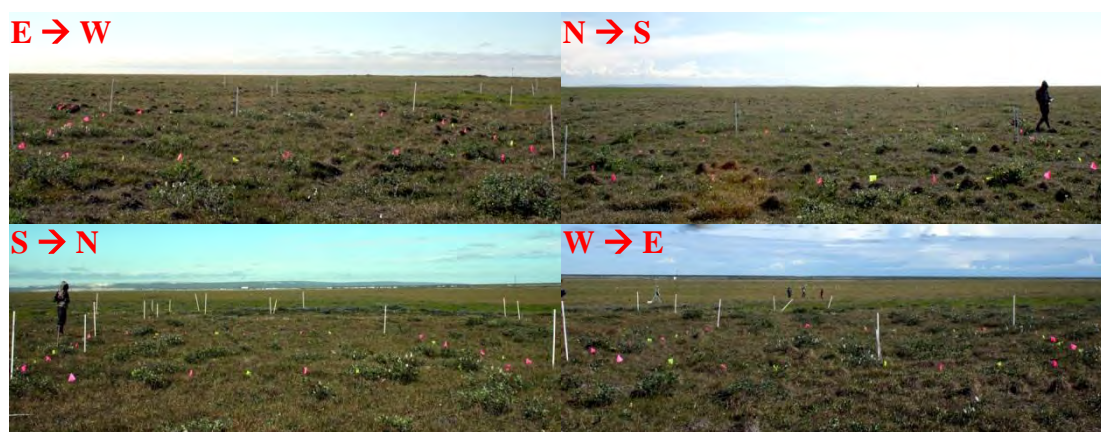


Figure C.2-3: Overview images of MNT tundra at the mesic Franklin Bluffs study location near the FBG2 site. Source: [Buchhorn and Schwieder, 2012]

III *Vegetation Description of the FBG2 Site*

The focus of the measurements at this goniometer site has been prostrate dwarf deciduous shrubs (*Salix*). The 1 x 1 m plot is homogeneously covered mainly with *Salix*, but with forbs, mosses and lichens in the understory.



Figure C.2-4: Overview images of the FBG2 vegetation from cardinal directions.



Figure C.2-5: Nadir image of the FBG2 vegetation (prostrate dwarf shrub).

IV *Overview of the Spectro-Goniometer Measurements*

Table C.2-1: Overview of the spectro-goniometer measurements at the FBG2 study site.

| Name | Day | Starting Time | Duration | SAA | SZA | Sky |
|---------|------------|---------------|----------|------|-----|--------------|
| FBG2_01 | 2012-07-09 | 09:39:42 | 18 min | 107° | 60° | cirrostratus |
| FBG2_02 | 2012-07-09 | 12:04:07 | 19 min | 146° | 50° | cirrostratus |
| FBG2_03 | 2012-07-09 | 13:48:12 | 25 min | 180° | 47° | cirrostratus |

Table C.2-3: Spectro-directional data of the FBG2_02 spectro-goniometer measurement.

| FBG2_02 (SZA = 50°; SAA = 146°) | | Viewing Geometry (Viewing Zenith Angle Viewing Azimuth Angle) | | | | | | | | | | | | | | | | | | | |
|------------------------------------|--------|---|--------|---------|--------|--------|--------|---------|--------|--------|--------|--------|--------|--------|--------|----------|--------|--------|--------|----------|--------|
| | | 010 | 5180 | 51202.5 | 51225 | 51270 | 51315 | 51337.5 | 510 | 5145 | 5190 | 51335 | 5157.5 | 10180 | 101190 | 101202.5 | 101225 | 101270 | 101315 | 101337.5 | 101350 |
| HCRF EnMAP blue (479 nm) | 0.0417 | 0.0500 | 0.0389 | 0.0437 | 0.0431 | 0.0440 | 0.0371 | 0.0437 | 0.0414 | 0.0445 | 0.0371 | 0.0363 | 0.0399 | 0.0513 | 0.0467 | 0.0436 | 0.0471 | 0.0422 | 0.0438 | 0.0381 | 0.0384 |
| HCRF EnMAP green (549 nm) | 0.0655 | 0.0788 | 0.0622 | 0.0705 | 0.0639 | 0.0659 | 0.0587 | 0.0688 | 0.0668 | 0.0688 | 0.0688 | 0.0658 | 0.0650 | 0.0819 | 0.0744 | 0.0697 | 0.0754 | 0.0635 | 0.0627 | 0.0612 | 0.0513 |
| HCRF EnMAP rot (672 nm) | 0.0554 | 0.0632 | 0.0520 | 0.0572 | 0.0632 | 0.0633 | 0.0493 | 0.0595 | 0.0556 | 0.0573 | 0.0481 | 0.0494 | 0.0515 | 0.0652 | 0.0620 | 0.0583 | 0.0617 | 0.0607 | 0.0628 | 0.0506 | 0.0604 |
| HCRF EnMAP NIR (864 nm) | 0.3197 | 0.3438 | 0.3017 | 0.3462 | 0.2650 | 0.2859 | 0.2815 | 0.3407 | 0.3321 | 0.3273 | 0.3102 | 0.2592 | 0.3276 | 0.3601 | 0.3320 | 0.3228 | 0.3373 | 0.2861 | 0.2594 | 0.3147 | 0.3211 |
| ANIF EnMAP rot (672 nm) | 1.0000 | 1.1408 | 0.9379 | 1.0319 | 1.1400 | 1.1413 | 0.8899 | 1.0740 | 1.0029 | 1.0332 | 0.8670 | 0.8904 | 0.9298 | 1.1769 | 1.1187 | 1.0525 | 1.1134 | 1.0952 | 1.1321 | 0.9123 | 0.9088 |
| ANIF EnMAP NIR (864 nm) | 1.0000 | 1.0754 | 0.9436 | 1.0830 | 0.8288 | 0.8943 | 0.8805 | 1.0657 | 1.0386 | 1.0237 | 0.9701 | 0.8014 | 1.0246 | 1.1262 | 1.0384 | 1.0096 | 1.0551 | 0.9323 | 0.8114 | 0.9844 | 1.0045 |
| Rel. Blue Absorption Depth | 0.3551 | 0.3701 | 0.3639 | 0.3747 | 0.3135 | 0.3224 | 0.3598 | 0.3508 | 0.3808 | 0.3437 | 0.3867 | 0.3140 | 0.3800 | 0.3768 | 0.3778 | 0.3652 | 0.3786 | 0.3261 | 0.2806 | 0.3741 | 0.3056 |
| Rel. Red Absorption Depth | 1.8552 | 1.7118 | 1.8439 | 1.9628 | 1.2223 | 1.3496 | 1.7848 | 1.8267 | 1.9373 | 1.8249 | 2.1164 | 1.5825 | 2.0630 | 1.7545 | 1.6840 | 1.7659 | 1.7375 | 1.2769 | 1.1956 | 1.9851 | 2.0754 |
| NDVI (EnMAP) | 0.7045 | 0.6893 | 0.7060 | 0.7164 | 0.6149 | 0.6376 | 0.7018 | 0.7025 | 0.7132 | 0.7021 | 0.7317 | 0.6789 | 0.7281 | 0.6832 | 0.6852 | 0.6938 | 0.6906 | 0.6285 | 0.6104 | 0.7231 | 0.7288 |
| Nadir Norm. NDVI (AVHRR) | 1.0000 | 0.9619 | 0.9987 | 1.0169 | 0.8875 | 0.9114 | 0.9909 | 0.9981 | 1.0069 | 0.9924 | 1.0282 | 0.9632 | 1.0240 | 0.9693 | 0.9675 | 0.9804 | 0.9748 | 0.9014 | 0.8760 | 1.0221 | 1.0234 |
| Nadir Norm. NDVI (MODIS) | 1.0000 | 0.9645 | 0.9981 | 1.0167 | 0.8851 | 0.9098 | 0.9923 | 0.9979 | 1.0075 | 0.9926 | 1.0292 | 0.9623 | 1.0233 | 0.9714 | 0.9688 | 0.9817 | 0.9757 | 0.8986 | 0.8750 | 1.0224 | 1.0246 |
| Nadir Norm. NDVI (EnMAP) | 1.0000 | 0.9785 | 1.0021 | 1.0170 | 0.8728 | 0.9051 | 0.9962 | 0.9972 | 1.0123 | 0.9967 | 1.0386 | 0.9609 | 1.0335 | 0.9840 | 0.9727 | 0.9849 | 0.9804 | 0.8921 | 0.8665 | 1.0265 | 1.0346 |

(cont.)

| FBG2_02 (SZA = 50°; SAA = 146°) | | Viewing Geometry (Viewing Zenith Angle Viewing Azimuth Angle) | | | | | | | | | | | | | | | | | | | |
|------------------------------------|--------|---|--------|---------|--------|--------|--------|---------|--------|--------|--------|----------|--------|--------|--------|----------|--------|--------|--------|---------|--------|
| | | 1010 | 10110 | 10122.5 | 10145 | 10190 | 10135 | 10157.5 | 101170 | 20180 | 20190 | 201202.5 | 201225 | 201270 | 201315 | 201337.5 | 201350 | 2010 | 20110 | 20122.5 | 20145 |
| HCRF EnMAP blue (479 nm) | 0.0434 | 0.0385 | 0.0431 | 0.0357 | 0.0378 | 0.0382 | 0.0404 | 0.0507 | 0.0433 | 0.0441 | 0.0470 | 0.0455 | 0.0439 | 0.0336 | 0.0368 | 0.0379 | 0.0418 | 0.0388 | 0.0388 | 0.0331 | 0.0351 |
| HCRF EnMAP green (549 nm) | 0.0687 | 0.0619 | 0.0674 | 0.0574 | 0.0610 | 0.0574 | 0.0658 | 0.0828 | 0.0707 | 0.0742 | 0.0768 | 0.0708 | 0.0660 | 0.0562 | 0.0577 | 0.0600 | 0.0636 | 0.0588 | 0.0592 | 0.0503 | 0.0553 |
| HCRF EnMAP rot (672 nm) | 0.0598 | 0.0506 | 0.0550 | 0.0447 | 0.0497 | 0.0508 | 0.0522 | 0.0635 | 0.0594 | 0.0602 | 0.0605 | 0.0592 | 0.0611 | 0.0462 | 0.0495 | 0.0503 | 0.0571 | 0.0527 | 0.0512 | 0.0439 | 0.0490 |
| HCRF EnMAP NIR (864 nm) | 0.3172 | 0.3251 | 0.3240 | 0.2790 | 0.2996 | 0.2812 | 0.3338 | 0.3718 | 0.3306 | 0.3511 | 0.3503 | 0.3139 | 0.2853 | 0.3007 | 0.2878 | 0.3089 | 0.3045 | 0.2801 | 0.2755 | 0.2483 | 0.2805 |
| ANIF EnMAP rot (672 nm) | 1.0794 | 0.9125 | 0.9920 | 0.8676 | 0.9370 | 0.9156 | 0.9416 | 1.1456 | 1.0708 | 1.0864 | 1.0918 | 1.0676 | 1.1025 | 0.8342 | 0.8929 | 0.9067 | 1.0294 | 0.9500 | 0.9235 | 0.7928 | 0.8832 |
| ANIF EnMAP NIR (864 nm) | 0.9920 | 1.0168 | 1.0134 | 0.8027 | 0.9370 | 0.9170 | 0.9441 | 1.1631 | 1.0340 | 1.0982 | 1.0956 | 0.9819 | 0.8924 | 0.9405 | 0.9003 | 0.9660 | 1.0284 | 0.8762 | 0.8616 | 0.7768 | 0.8773 |
| Rel. Blue Absorption Depth | 0.3315 | 0.3669 | 0.3526 | 0.3737 | 0.3722 | 0.3102 | 0.3781 | 0.4009 | 0.3850 | 0.4141 | 0.3943 | 0.3475 | 0.3226 | 0.4018 | 0.3490 | 0.3512 | 0.3222 | 0.3156 | 0.3250 | 0.3177 | 0.3570 |
| Rel. Red Absorption Depth | 1.6499 | 2.0691 | 1.9030 | 2.0058 | 1.9333 | 1.5717 | 1.8974 | 1.7745 | 1.8388 | 1.6653 | 1.6653 | 1.3805 | 2.0988 | 1.8585 | 2.0048 | 1.6731 | 1.6507 | 1.6807 | 1.6807 | 1.7627 | 1.7978 |
| NDVI (EnMAP) | 0.6826 | 0.7307 | 0.7098 | 0.7237 | 0.7152 | 0.6746 | 0.7295 | 0.7083 | 0.6955 | 0.7072 | 0.7053 | 0.6828 | 0.6472 | 0.7334 | 0.7066 | 0.7201 | 0.6944 | 0.6835 | 0.6865 | 0.6993 | 0.7028 |
| Nadir Norm. NDVI (AVHRR) | 0.9694 | 1.0368 | 1.0024 | 1.0191 | 1.0083 | 0.9506 | 1.0252 | 0.9883 | 0.9778 | 0.9867 | 0.9897 | 0.9621 | 0.9248 | 1.0389 | 0.9885 | 1.0194 | 0.9697 | 0.9736 | 0.9747 | 0.9950 | 1.0024 |
| Nadir Norm. NDVI (MODIS) | 0.9701 | 1.0374 | 1.0039 | 1.0197 | 1.0087 | 0.9513 | 1.0244 | 0.9907 | 0.9772 | 0.9869 | 0.9919 | 0.9619 | 0.9230 | 1.0387 | 1.0003 | 1.0199 | 0.9698 | 0.9743 | 0.9754 | 0.9950 | 1.0010 |
| Nadir Norm. NDVI (EnMAP) | 0.9689 | 1.0372 | 1.0076 | 1.0273 | 1.0152 | 0.9576 | 1.0356 | 1.0054 | 0.9873 | 1.0038 | 1.0013 | 0.9692 | 0.9186 | 1.0411 | 1.0030 | 1.0221 | 0.9715 | 0.9703 | 0.9746 | 0.9927 | 0.9976 |

(cont.)

| FBG2_02 (SZA = 50°; SAA = 146°) | | Viewing Geometry (Viewing Zenith Angle Viewing Azimuth Angle) | | | | | | | | | | | | | | | | | | | |
|------------------------------------|--------|---|----------|--------|--------|--------|----------|--------|--------|--------|----------|--------|--------|--------|---------|--------|--------|--------|---------|--------|--------|
| | | 20135 | 201157.5 | 201170 | 30180 | 30180 | 301202.5 | 301225 | 301270 | 301315 | 301337.5 | 301350 | 3010 | 30110 | 30122.5 | 30145 | 30190 | 30135 | 30157.5 | 301170 | 30135 |
| HCRF EnMAP blue (479 nm) | 0.0436 | 0.0451 | 0.0419 | 0.0635 | 0.0679 | 0.0625 | 0.0470 | 0.0379 | 0.0354 | 0.0367 | 0.0310 | 0.0287 | 0.0302 | 0.0332 | 0.0328 | 0.0423 | 0.0491 | 0.0535 | 0.0624 | 0.0624 | 0.0624 |
| HCRF EnMAP green (549 nm) | 0.0662 | 0.0711 | 0.0665 | 0.0998 | 1.052 | 0.992 | 0.733 | 0.0588 | 0.0571 | 0.0538 | 0.0482 | 0.0455 | 0.0456 | 0.0509 | 0.0511 | 0.0671 | 0.0750 | 0.0863 | 0.0960 | 0.0960 | 0.0960 |
| HCRF EnMAP rot (672 nm) | 0.0578 | 0.0594 | 0.0547 | 0.0814 | 0.0885 | 0.0790 | 0.0586 | 0.0504 | 0.0489 | 0.0515 | 0.0438 | 0.0393 | 0.0421 | 0.0462 | 0.0449 | 0.0551 | 0.0647 | 0.0703 | 0.0813 | 0.0813 | 0.0813 |
| HCRF EnMAP NIR (864 nm) | 0.2796 | 0.3261 | 0.3124 | 0.3124 | 0.3849 | 0.4021 | 0.3919 | 0.3041 | 0.2841 | 0.2886 | 0.2497 | 0.2408 | 0.2368 | 0.2175 | 0.2327 | 0.2496 | 0.3376 | 0.3366 | 0.3930 | 0.3851 | 0.3851 |
| ANIF EnMAP rot (672 nm) | 1.0428 | 1.0719 | 0.9862 | 1.4685 | 1.5986 | 1.4258 | 1.0574 | 0.9098 | 0.8814 | 0.9283 | 0.7907 | 0.7093 | 0.7801 | 0.8334 | 0.8099 | 0.9940 | 1.1675 | 1.2674 | 1.4666 | 1.4666 | 1.4666 |
| ANIF EnMAP NIR (864 nm) | 0.8651 | 1.0198 | 0.9773 | 1.2039 | 1.2577 | 1.2259 | 0.9510 | 0.8887 | 0.9026 | 0.7812 | 0.7531 | 0.7405 | 0.6803 | 0.7280 | 0.7807 | 1.0559 | 1.0528 | 1.2293 | 1.2044 | 1.2044 | 1.2044 |
| Rel. Blue Absorption Depth | 0.3198 | 0.3533 | 0.3548 | 0.3629 | 0.3540 | 0.3780 | 0.3490 | 0.3459 | 0.3780 | 0.2933 | 0.3442 | 0.3505 | 0.3153 | 0.3320 | 0.3388 | 0.3591 | 0.3259 | 0.3675 | 0.3386 | 0.3386 | 0.3386 |
| Rel. Red Absorption Depth | 1.4534 | 1.7320 | 1.8176 | 1.4585 | 1.3648 | 1.5355 | 1.5722 | 1.7465 | 1.8963 | 1.6961 | 1.6961 | 1.8788 | 1.5788 | 1.5118 | 1.7130 | 1.9858 | 1.6546 | 1.7976 | 1.4722 | 1.4722 | 1.4722 |
| NDVI (EnMAP) | 0.6542 | 0.6917 | 0.7021 | 0.6508 | 0.6393 | 0.6644 | 0.6767 | 0.6985 | 0.7104 | 0.6583 | 0.6920 | 0.7152 | 0.6754 | 0.6687 | 0.6951 | 0.7193 | 0.6675 | 0.6967 | 0.6513 | 0.6513 | 0.6513 |
| Nadir Norm. NDVI (AVHRR) | 0.9234 | 0.9710 | 0.9821 | 0.9064 | 0.8885 | 0.9206 | 0.9393 | 0.9893 | 1.0123 | 0.9470 | 0.9901 | 1.0203 | 0.9640 | 0.9536 | 0.9894 | 1.0119 | 0.9541 | 0.9774 | 0.9116 | 0.9116 | 0.9116 |
| Nadir Norm. NDVI (MODIS) | 0.9249 | 0.9718 | 0.9827 | 0.9115 | 0.8928 | 0.9254 | 0.9442 | 0.9898 | 1.0138 | 0.9470 | 0.9901 | 1.0194 | 0.9637 | 0.9553 | 0.9940 | 1.0139 | 0.9550 | 0.9790 | 0.9146 | 0.9146 | 0.9146 |
| Nadir Norm. NDVI (EnMAP) | 0.9287 | 0.9819 | 0.9967 | 0.9239 | 0.9076 | 0.9431 | 0.9607 | 0.9915 | 1.0084 | 0.9345 | 0.9823 | 1.0152 | 0.9588 | 0.9493 | 0.9867 | 1.0211 | 0.9617 | 0.9890 | 0.9246 | 0.9246 | 0.9246 |

Table C.2-4: Spectro-directional data of the FBG2_03 spectro-goniometer measurement

| FBG2_03 (SA = 47°; SAA = 180°) | | Viewing Geometry (Viewing Zenith Angle Viewing Azimuth Angle) | | | | | | | | | | | | | | | | | | | | | | | | | | | | | | | | | | | | | | | | | | |
|-----------------------------------|--------|---|--------|---------|--------|--------|--------|---------|--------|--------|--------|--------|--------|---------|--------|--------|----------|--------|--------|--------|----------|--------|--------|--------|--------|--------|--------|--------|--------|--------|--------|--------|--------|--------|--------|--------|--------|--------|--------|--------|--------|--------|--------|--------|
| | | 0 0 | 5 180 | 5 202.5 | 5 225 | 5 270 | 5 315 | 5 337.5 | 5 0 | 5 22.5 | 5 45 | 5 90 | 5 135 | 5 157.5 | 10 180 | 10 190 | 10 202.5 | 10 225 | 10 270 | 10 315 | 10 337.5 | 10 350 | | | | | | | | | | | | | | | | | | | | | | |
| HCRF EnMAP blue (479 nm) | 0.0461 | 0.0493 | 0.0433 | 0.0443 | 0.0472 | 0.0438 | 0.0440 | 0.0458 | 0.0442 | 0.0478 | 0.0486 | 0.0501 | 0.0529 | 0.0549 | 0.0424 | 0.0429 | 0.0471 | 0.0393 | 0.0425 | 0.0428 | 0.0410 | 0.0384 | 0.0394 | 0.0465 | 0.0499 | 0.0711 | 0.0794 | 0.0651 | 0.0659 | 0.0672 | 0.0701 | 0.0735 | 0.0783 | 0.0872 | 0.0748 | 0.0490 | 0.0440 | 0.0437 | 0.0386 | 0.0412 | 0.0375 | 0.0377 | 0.0391 | 0.0427 |
| HCRF EnMAP green (549 nm) | 0.0723 | 0.0749 | 0.0745 | 0.0644 | 0.0665 | 0.0743 | 0.0681 | 0.0678 | 0.0717 | 0.0681 | 0.0740 | 0.0736 | 0.0755 | 0.0824 | 0.0825 | 0.0657 | 0.0648 | 0.0708 | 0.0657 | 0.0668 | 0.0659 | 0.0642 | 0.0598 | 0.0549 | 0.0644 | 0.0651 | 0.0627 | 0.0644 | 0.0659 | 0.0672 | 0.0701 | 0.0735 | 0.0783 | 0.0872 | 0.0748 | 0.0490 | 0.0440 | 0.0437 | 0.0386 | 0.0412 | 0.0375 | 0.0377 | 0.0391 | 0.0427 |
| HCRF EnMAP rot (672 nm) | 0.0620 | 0.0696 | 0.0672 | 0.0606 | 0.0627 | 0.0645 | 0.0571 | 0.0582 | 0.0617 | 0.0634 | 0.0606 | 0.0621 | 0.0679 | 0.0703 | 0.0643 | 0.0657 | 0.0683 | 0.0643 | 0.0679 | 0.0686 | 0.0566 | 0.0563 | 0.0529 | 0.0549 | 0.0644 | 0.0651 | 0.0627 | 0.0644 | 0.0659 | 0.0672 | 0.0701 | 0.0735 | 0.0783 | 0.0872 | 0.0748 | 0.0490 | 0.0440 | 0.0437 | 0.0386 | 0.0412 | 0.0375 | 0.0377 | 0.0391 | 0.0427 |
| HCRF EnMAP NIR (864 nm) | 0.3600 | 0.3214 | 0.3241 | 0.3241 | 0.2729 | 0.2892 | 0.3099 | 0.3342 | 0.3419 | 0.3152 | 0.3425 | 0.3159 | 0.3430 | 0.3200 | 0.3624 | 0.3472 | 0.2975 | 0.2838 | 0.3356 | 0.3218 | 0.3379 | 0.1336 | 0.9080 | 0.8535 | 0.8854 | 1.0387 | 1.0506 | 1.0631 | 0.8824 | 1.1299 | 1.1854 | 1.2142 | 1.0838 | 0.9600 | 0.9708 | 0.8441 | 0.9089 | 0.8053 | 0.8315 | 0.8255 | 0.8158 | 0.8296 | 0.8705 | |
| ANIF EnMAP rot (672 nm) | 1.0000 | 1.1222 | 1.0842 | 0.9769 | 1.0112 | 1.0404 | 0.9213 | 0.9381 | 0.9959 | 1.0233 | 0.9771 | 1.0021 | 1.0858 | 1.1347 | 1.1879 | 1.2323 | 0.9720 | 0.9806 | 1.0367 | 0.8351 | 0.8992 | 0.9659 | 0.8973 | 0.8327 | 0.8664 | 1.0387 | 1.0506 | 1.0631 | 0.8824 | 1.1299 | 1.1854 | 1.2142 | 1.0838 | 0.9600 | 0.9708 | 0.8441 | 0.9089 | 0.8053 | 0.8315 | 0.8255 | 0.8158 | 0.8296 | 0.8705 | |
| ANIF EnMAP NIR (864 nm) | 1.0000 | 0.8927 | 0.9003 | 0.7579 | 0.8032 | 1.0274 | 0.9282 | 0.9498 | 0.8755 | 0.8774 | 0.9528 | 0.8911 | 0.8887 | 1.0065 | 0.9541 | 0.9329 | 0.8264 | 0.7882 | 0.9321 | 0.8938 | 0.9386 | 0.3531 | 0.3368 | 0.3278 | 0.3144 | 0.3203 | 0.3589 | 0.3441 | 0.3378 | 0.3308 | 0.3426 | 0.3241 | 0.3541 | 0.3249 | 0.3492 | 0.3190 | 0.3140 | 0.3640 | 0.3517 | | | | | |
| Rel. Blue Absorption Depth | 1.8593 | 1.3916 | 1.4657 | 1.3226 | 1.3625 | 1.8396 | 1.8819 | 1.8768 | 1.5965 | 1.7002 | 1.6282 | 1.7392 | 1.4351 | 1.3746 | 1.5195 | 1.3721 | 1.5117 | 1.4023 | 1.6246 | 1.9914 | 1.9525 | 0.7082 | 0.6441 | 0.6565 | 0.6367 | 0.7030 | 0.7080 | 0.7092 | 0.6724 | 0.6874 | 0.6781 | 0.6933 | 0.6505 | 0.6395 | 0.6622 | 0.6393 | 0.6631 | 0.6471 | 0.6785 | 0.7228 | 0.7168 | | | |
| Nadir Norm. NDVI (AVHRR) | 1.0000 | 0.9164 | 0.9334 | 0.9064 | 0.9141 | 0.9970 | 1.0045 | 1.0035 | 0.9575 | 0.9775 | 0.9644 | 0.9789 | 0.9255 | 0.9128 | 0.9464 | 0.9126 | 0.9504 | 0.9232 | 0.9631 | 1.0243 | 1.0174 | 1.0000 | 0.9146 | 0.9322 | 0.9055 | 0.9140 | 0.9972 | 1.0052 | 1.0039 | 0.9564 | 0.9779 | 0.9636 | 0.9801 | 0.9242 | 0.9108 | 0.9442 | 0.9123 | 0.9496 | 0.9217 | 0.9642 | 1.0255 | 1.0175 | | |
| Nadir Norm. NDVI (MODIS) | 1.0000 | 0.9120 | 0.9296 | 0.9016 | 0.9114 | 0.9955 | 1.0026 | 1.0044 | 0.9521 | 0.9734 | 0.9603 | 0.9818 | 0.9211 | 0.9056 | 0.9377 | 0.9053 | 0.9390 | 0.9164 | 0.9608 | 1.0236 | 1.0150 | 1.0000 | 0.9120 | 0.9296 | 0.9016 | 0.9114 | 0.9955 | 1.0026 | 1.0044 | 0.9521 | 0.9734 | 0.9603 | 0.9818 | 0.9211 | 0.9056 | 0.9377 | 0.9053 | 0.9390 | 0.9164 | 0.9608 | 1.0236 | 1.0150 | | |
| Nadir Norm. NDVI (EnMAP) | | | | | | | | | | | | | | | | | | | | | | | | | | | | | | | | | | | | | | | | | | | | |

(cont.)

| FBG2_03 (SA = 47°; SAA = 180°) | | Viewing Geometry (Viewing Zenith Angle Viewing Azimuth Angle) | | | | | | | | | | | | | | | | | | | | |
|-----------------------------------|--------|---|--------|---------|--------|--------|--------|----------|--------|--------|--------|----------|--------|--------|--------|----------|--------|--------|--------|---------|--------|-------|
| | | 10 0 | 10 10 | 10 22.5 | 10 45 | 10 90 | 10 135 | 10 157.5 | 10 170 | 20 180 | 20 190 | 20 202.5 | 20 225 | 20 270 | 20 315 | 20 337.5 | 20 350 | 20 0 | 20 10 | 20 22.5 | 20 45 | 20 90 |
| HCRF EnMAP blue (479 nm) | 0.0428 | 0.0410 | 0.0384 | 0.0394 | 0.0465 | 0.0477 | 0.0516 | 0.0530 | 0.0560 | 0.0477 | 0.0516 | 0.0530 | 0.0560 | 0.0440 | 0.0437 | 0.0386 | 0.0412 | 0.0375 | 0.0377 | 0.0391 | 0.0427 | |
| HCRF EnMAP green (549 nm) | 0.0659 | 0.0642 | 0.0598 | 0.0640 | 0.0711 | 0.0794 | 0.0735 | 0.0777 | 0.0783 | 0.0872 | 0.0748 | 0.0695 | 0.0688 | 0.0601 | 0.0523 | 0.0564 | 0.0499 | 0.0573 | 0.0581 | 0.0606 | 0.0584 | |
| HCRF EnMAP rot (672 nm) | 0.0566 | 0.0563 | 0.0529 | 0.0549 | 0.0644 | 0.0651 | 0.0659 | 0.0672 | 0.0701 | 0.0735 | 0.0783 | 0.0872 | 0.0748 | 0.0695 | 0.0601 | 0.0523 | 0.0564 | 0.0499 | 0.0573 | 0.0581 | 0.0606 | |
| HCRF EnMAP NIR (864 nm) | 0.3225 | 0.3230 | 0.3014 | 0.3207 | 0.3254 | 0.3806 | 0.3240 | 0.3177 | 0.3290 | 0.3150 | 0.3832 | 0.3253 | 0.3343 | 0.3495 | 0.2980 | 0.2885 | 0.2836 | 0.2861 | 0.3069 | 0.2937 | 0.2872 | |
| ANIF EnMAP rot (672 nm) | 0.9136 | 0.9080 | 0.8535 | 0.8854 | 1.0387 | 1.0506 | 1.0631 | 0.8824 | 1.1299 | 1.1854 | 1.2142 | 1.0838 | 0.9600 | 0.9708 | 0.8441 | 0.9089 | 0.8053 | 0.8315 | 0.8255 | 0.8158 | 0.8296 | |
| ANIF EnMAP NIR (864 nm) | 0.8959 | 0.8973 | 0.8327 | 0.8664 | 1.0387 | 1.0506 | 1.0631 | 0.8824 | 1.1299 | 1.1854 | 1.2142 | 1.0838 | 0.9600 | 0.9708 | 0.8441 | 0.9089 | 0.8053 | 0.8315 | 0.8255 | 0.8158 | 0.8296 | |
| Rel. Blue Absorption Depth | 0.3361 | 0.3454 | 0.3474 | 0.3851 | 0.3333 | 0.3643 | 0.3296 | 0.3390 | 0.3193 | 0.3103 | 0.3566 | 0.3306 | 0.3523 | 0.3515 | 0.3403 | 0.3153 | 0.3242 | 0.3250 | 0.3355 | 0.3305 | 0.3157 | |
| Rel. Red Absorption Depth | 1.7927 | 1.8028 | 1.7664 | 1.8399 | 1.5404 | 1.8800 | 1.5098 | 1.4380 | 1.4252 | 1.2566 | 1.5715 | 1.4601 | 1.7843 | 1.8419 | 1.7576 | 1.5421 | 1.7430 | 1.7174 | 1.7914 | 1.7877 | 1.4290 | |
| NDVI (EnMAP) | 0.7012 | 0.7032 | 0.7013 | 0.7077 | 0.6696 | 0.7077 | 0.6619 | 0.6510 | 0.6489 | 0.6216 | 0.6716 | 0.6578 | 0.6977 | 0.7064 | 0.6995 | 0.6732 | 0.7006 | 0.6947 | 0.7027 | 0.7020 | 0.6536 | |
| Nadir Norm. NDVI (AVHRR) | 0.9661 | 0.9977 | 1.0008 | 0.9677 | 0.9510 | 0.9990 | 0.9431 | 0.9277 | 0.9174 | 0.8798 | 0.9483 | 0.9310 | 0.9818 | 1.0026 | 0.9946 | 0.9601 | 0.9983 | 0.9872 | 0.9995 | 1.0002 | 0.9310 | |
| Nadir Norm. NDVI (MODIS) | 0.9955 | 0.9971 | 0.9997 | 1.0062 | 0.9497 | 0.9993 | 0.9419 | 0.9281 | 0.9175 | 0.8805 | 0.9494 | 0.9313 | 0.9935 | 1.0034 | 0.9957 | 0.9616 | 0.9990 | 0.9882 | 0.9994 | 0.9988 | 0.9305 | |
| Nadir Norm. NDVI (EnMAP) | 0.9930 | 0.9958 | 0.9931 | 1.0022 | 0.9481 | 1.0022 | 0.9373 | 0.9218 | 0.9189 | 0.8803 | 0.9510 | 0.9312 | 0.9881 | 1.0003 | 0.9906 | 0.9533 | 0.9922 | 0.9837 | 0.9951 | 0.9940 | 0.9255 | |

(cont.)

| FBG2_03 (SA = 47°; SAA = 180°) | | Viewing Geometry (Viewing Zenith Angle Viewing Azimuth Angle) | | | | | | | | | | | | | | | | | | | |
|-----------------------------------|--------|---|----------|--------|--------|--------|--------|--------|----------|--------|--------|--------|---------|--------|--------|--------|----------|--------|--|--|--|
| | | 20 135 | 20 157.5 | 20 170 | 30 180 | 30 190 | 30 225 | 30 315 | 30 337.5 | 30 350 | 30 0 | 30 10 | 30 22.5 | 30 45 | 30 90 | 30 135 | 30 157.5 | 30 170 | | | |
| HCRF EnMAP blue (479 nm) | 0.0579 | 0.0512 | 0.0549 | 0.0657 | 0.0651 | 0.0402 | 0.0367 | 0.0365 | 0.0358 | 0.0340 | 0.0322 | 0.0340 | 0.0447 | 0.0417 | 0.0541 | 0.0541 | 0.0586 | 0.0578 | | | |
| HCRF EnMAP green (549 nm) | 0.0887 | 0.0804 | 0.0857 | 0.1005 | 0.0967 | 0.0651 | 0.0570 | 0.0551 | 0.0540 | 0.0535 | 0.0507 | 0.0524 | 0.0709 | 0.0657 | 0.0837 | 0.0875 | 0.0869 | 0.0869 | | | |
| HCRF EnMAP rot (672 nm) | 0.0758 | 0.0650 | 0.0730 | 0.0875 | 0.0877 | 0.0542 | 0.0507 | 0.0503 | 0.0494 | 0.0469 | 0.0433 | 0.0458 | 0.0571 | 0.0573 | 0.0725 | 0.0725 | 0.0779 | 0.0786 | | | |
| HCRF EnMAP NIR (864 nm) | 0.3796 | 0.3676 | 0.3758 | 0.3762 | 0.3538 | 0.3801 | 0.3426 | 0.2799 | 0.2550 | 0.2549 | 0.2737 | 0.2698 | 0.2703 | 0.3637 | 0.3379 | 0.3603 | 0.3510 | 0.3385 | | | |
| ANIF EnMAP rot (672 nm) | 1.2222 | 1.0486 | 1.1775 | 1.4113 | 1.4153 | 1.3649 | 1.1907 | 0.8740 | 0.8185 | 0.7964 | 0.7589 | 0.6979 | 0.7390 | 0.9217 | 0.9240 | 1.1691 | 1.2559 | 1.2684 | | | |
| ANIF EnMAP NIR (864 nm) | 1.0545 | 1.0211 | 1.0438 | 1.0451 | 0.9828 | 1.0516 | 1.0559 | 0.9515 | 0.7083 | 0.7081 | 0.7602 | 0.7495 | 0.7507 | 1.0104 | 0.9386 | 1.0007 | 0.9751 | 0.9403 | | | |
| Rel. Blue Absorption Depth | 0.3373 | 0.3546 | 0.3479 | 0.3465 | 0.3208 | 0.3536 | 0.3670 | 0.3789 | 0.3457 | 0.3163 | 0.3148 | 0.3496 | 0.3419 | 0.3249 | 0.3513 | 0.3459 | 0.3085 | 0.3264 | | | |
| Rel. Red Absorption Depth | 1.5493 | 1.7686 | 1.5943 | 1.2613 | 1.1640 | 1.3205 | 1.1607 | 1.1992 | 1.7132 | 1.5245 | 1.7912 | 1.9593 | 1.8429 | 2.0462 | 1.8966 | 1.5331 | 1.3449 | 1.2521 | | | |
| NDVI (EnMAP) | 0.6672 | 0.6995 | 0.6746 | 0.6226 | 0.6026 | 0.6346 | 0.6747 | 0.7269 | 0.6931 | 0.6708 | 0.6755 | 0.7076 | 0.7101 | 0.7285 | 0.7101 | 0.6650 | 0.6369 | 0.6230 | | | |
| Nadir Norm. NDVI (AVHRR) | 0.9374 | 0.9800 | 0.9503 | 0.8714 | 0.8466 | 0.8975 | 0.9531 | 1.0306 | 0.9933 | 0.9555 | 0.9631 | 1.0112 | 1.0290 | 1.0123 | 1.0280 | 1.0145 | 0.9335 | 0.8940 | | | |
| Nadir Norm. NDVI (MODIS) | 0.9390 | 0.9820 | 0.9510 | 0.8740 | 0.8478 | 0.8979 | 0.9532 | 1.0315 | 0.9930 | 0.9565 | 0.9652 | 1.0122 | 1.0296 | 1.0119 | 1.0289 | 1.0133 | 0.9365 | 0.8967 | | | |
| Nadir Norm. NDVI (EnMAP) | 0.9448 | 0.9905 | 0.9554 | 0.8817 | 0.8533 | 0.8987 | 0.9555 | 1.0293 | 0.9815 | 0.9498 | 0.9565 | 1.0020 | 1.0247 | 1.0055 | 1.0316 | 1.0056 | 0.9417 | 0.9019 | | | |

V Main Spectral Characteristics

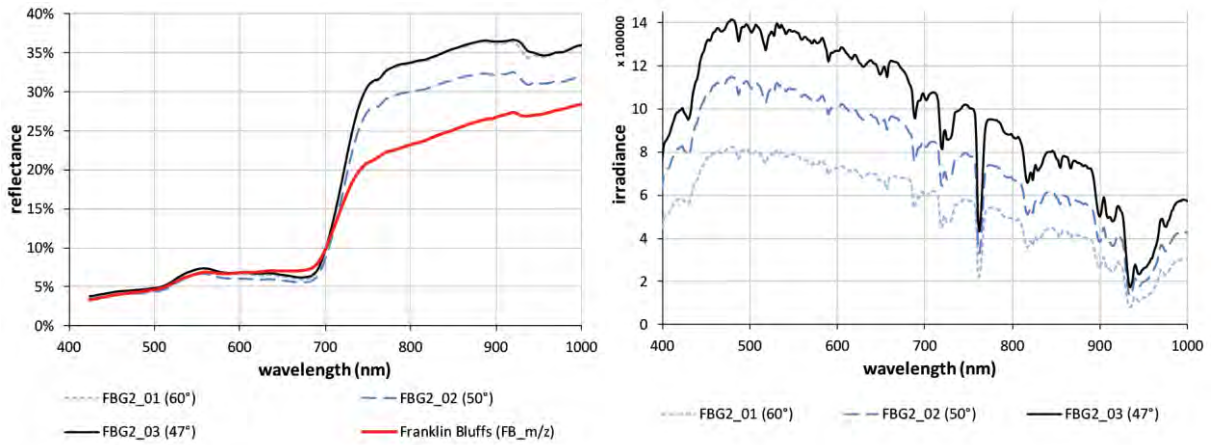


Figure C.2-6: Nadir reflectances and irradiance profiles of the FBG2 site at different sun zenith angles. Left: Comparison of the nadir reflectance signatures with the average zonal vegetation (MNT). Right: Comparison of the total irradiance profiles.

VI HCRF Visualization

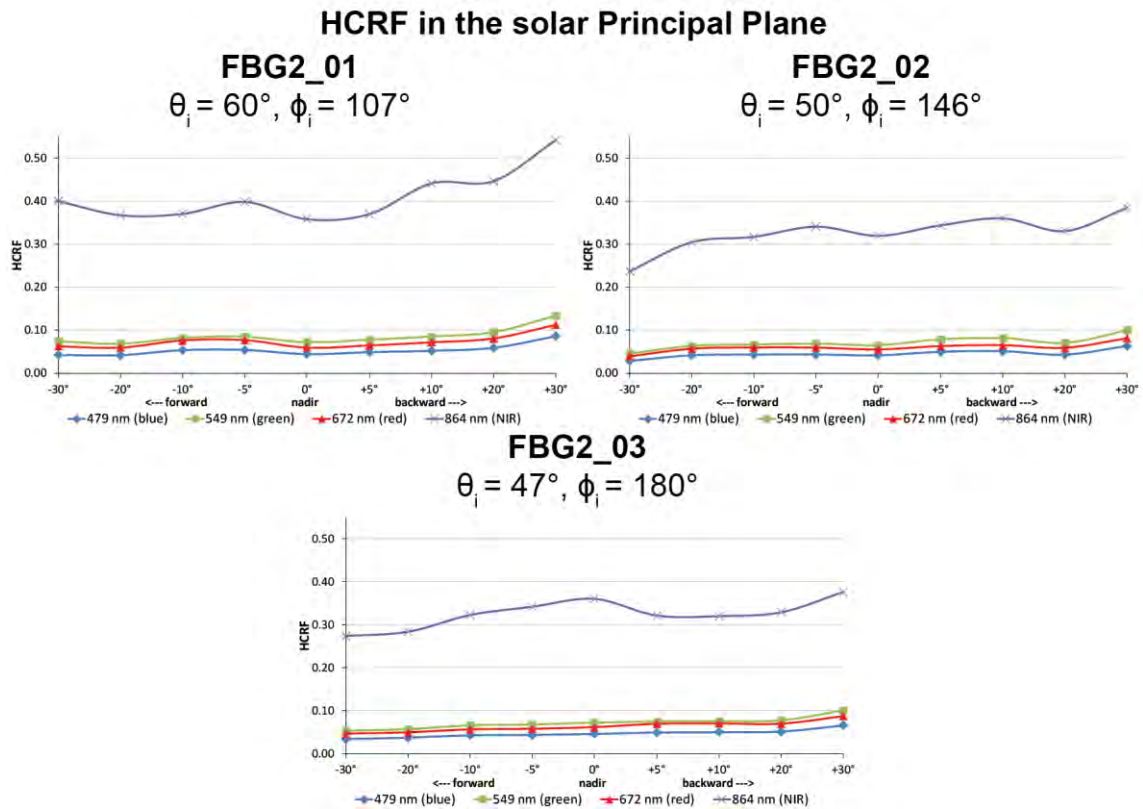


Figure C.2-7: Comparison of the HCRF values at 479 nm (blue), 549 nm (green), 672 nm (red), and 864 nm (NIR) in the solar principal plane of the FBG2 site at different sun zenith angles.

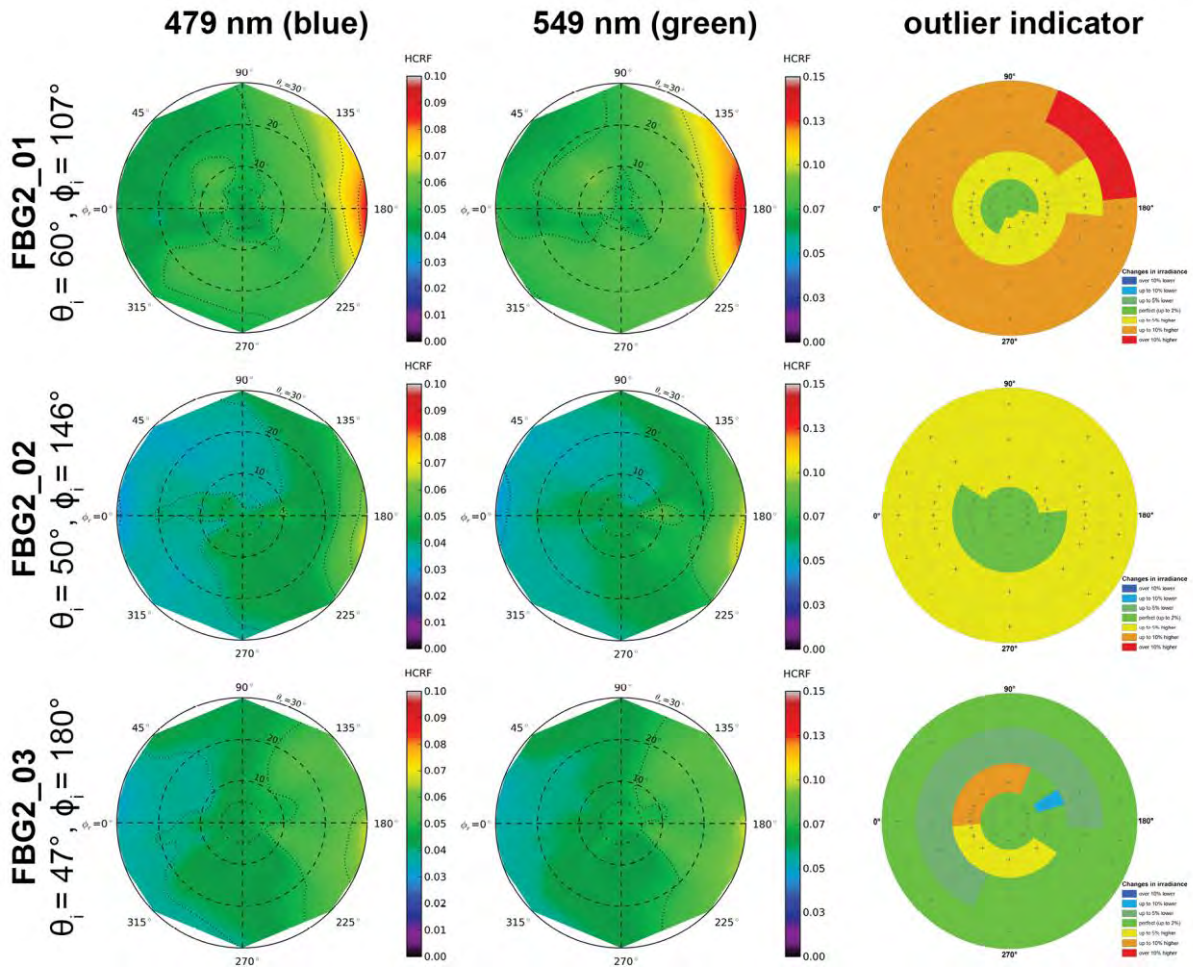


Figure C.2-8: HCRF visualization at 479 nm and 549 nm of the FBG2 site.

Changes in irradiance



Figure C.2-9: Legend of the outlier indicator graphics shown in Figure C.2-8, C.2-10, and C.2-13

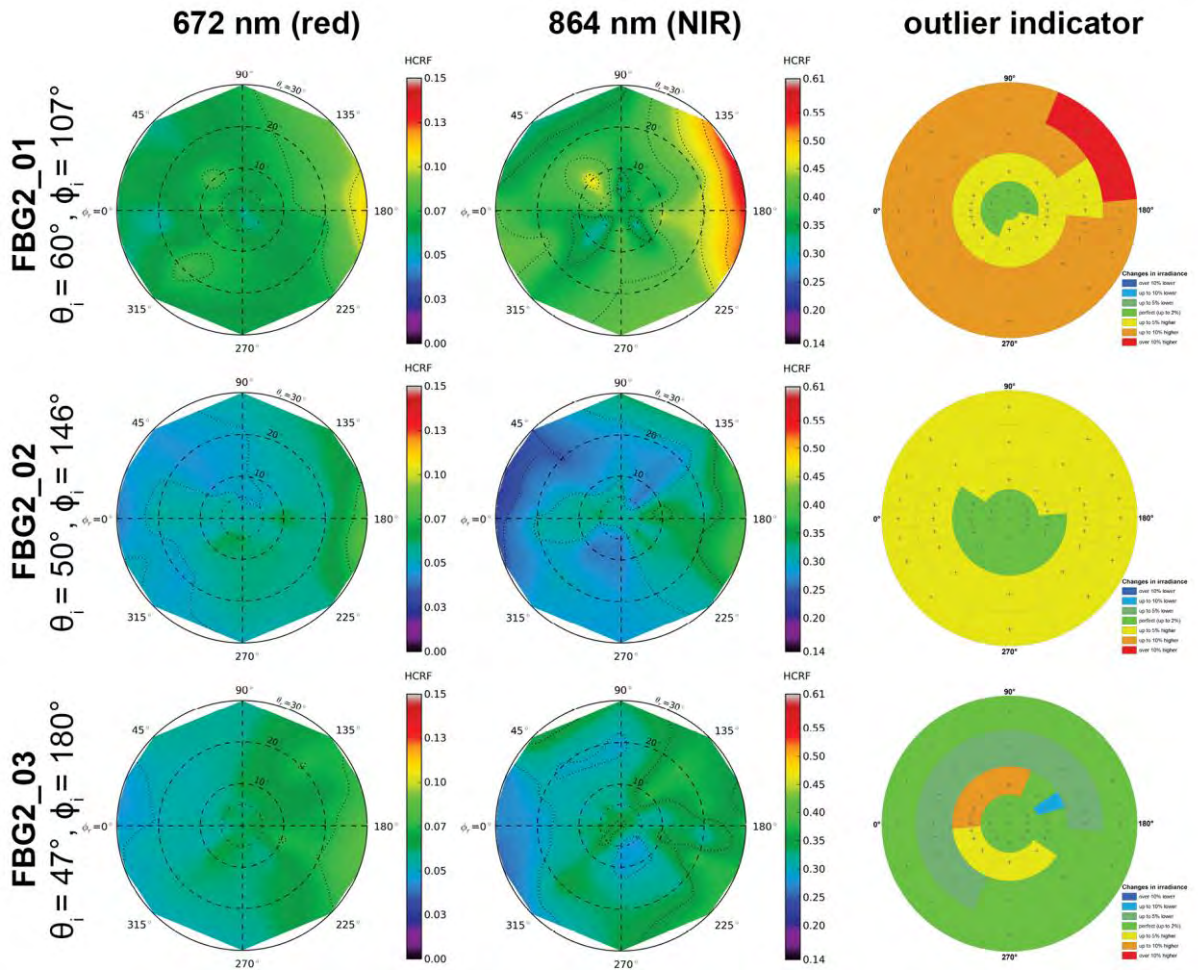


Figure C.2-10: HCRF visualization at 672 nm and 864 nm of the FBG2 site.

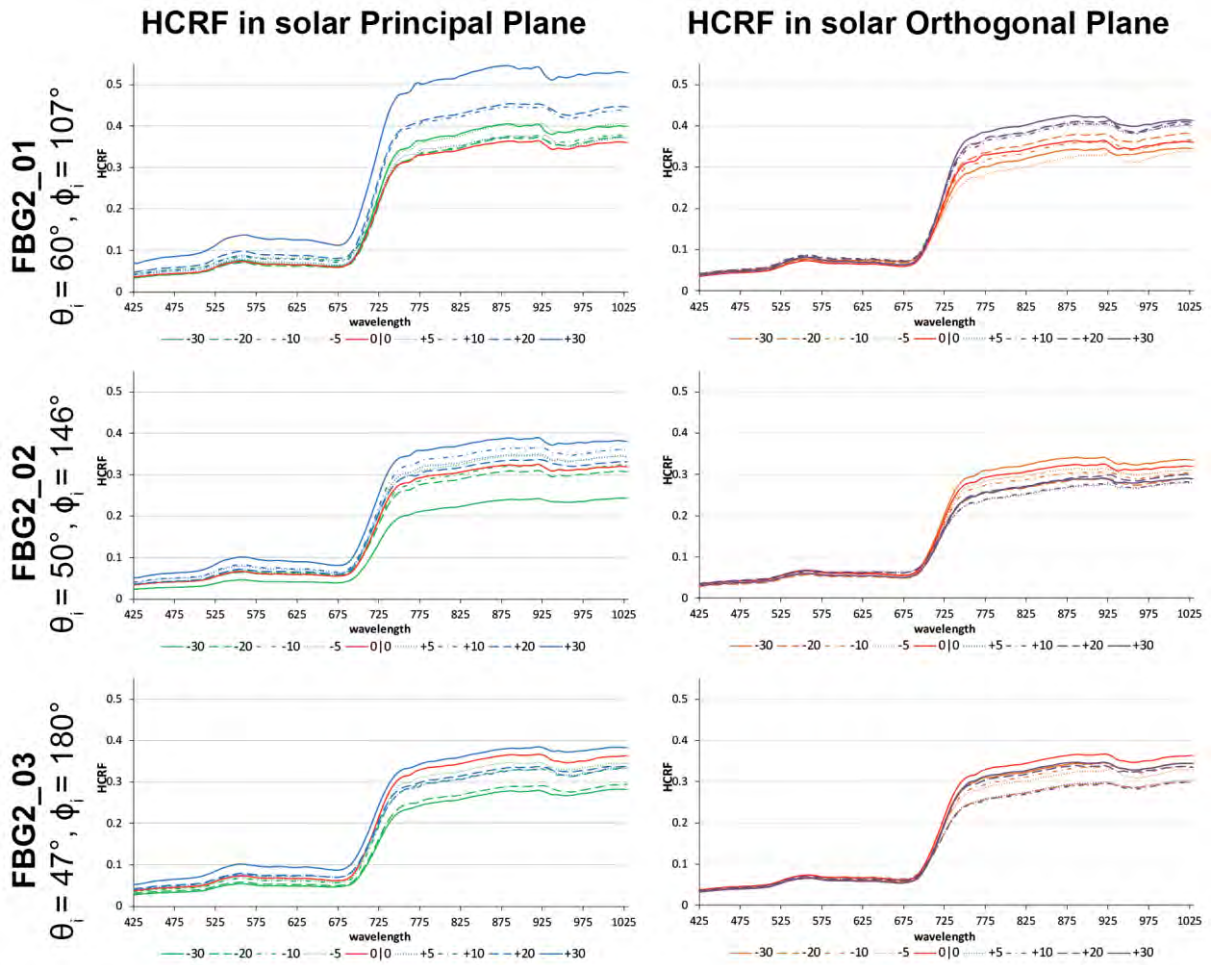


Figure C.2-11: HCRF visualization in principal & orthogonal plane of the FBG2 site.

VII ANIF Visualization

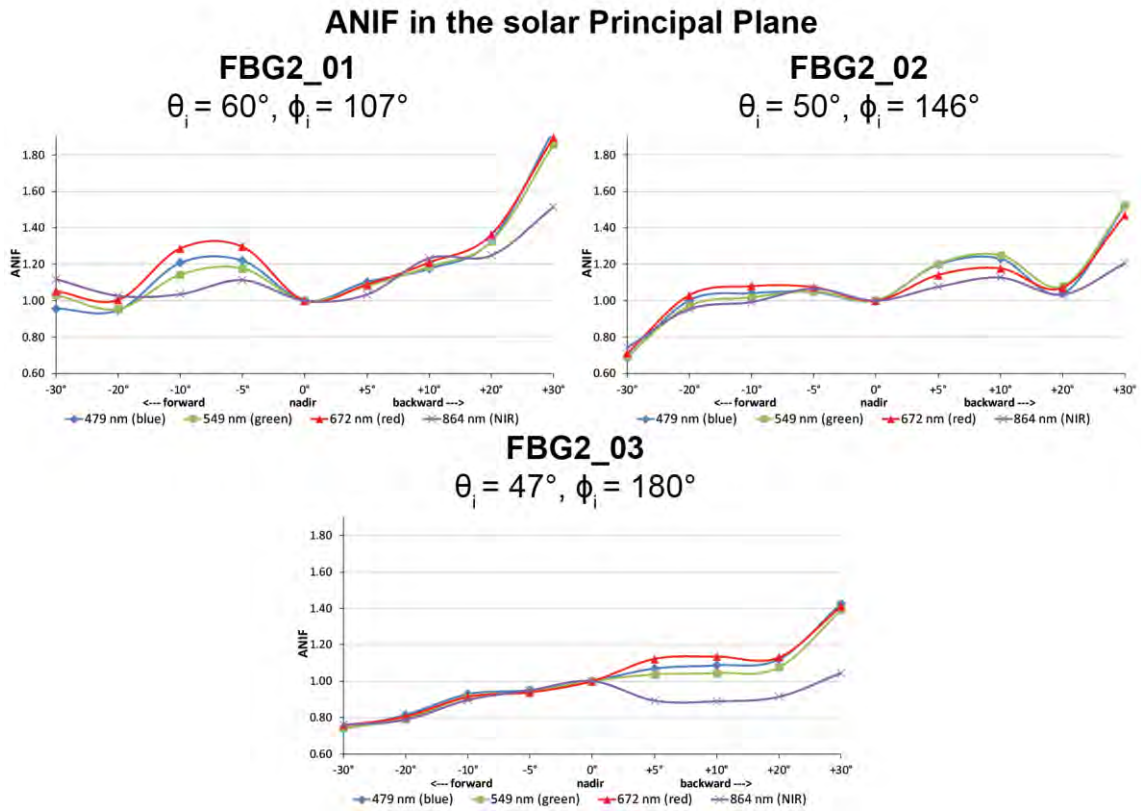


Figure C.2-12: Comparison of the ANIF values at 479 nm (blue), 549 nm (green), 672 nm (red), and 864 nm (NIR) in the solar principal plane of the FBG2 site at different sun zenith angles.

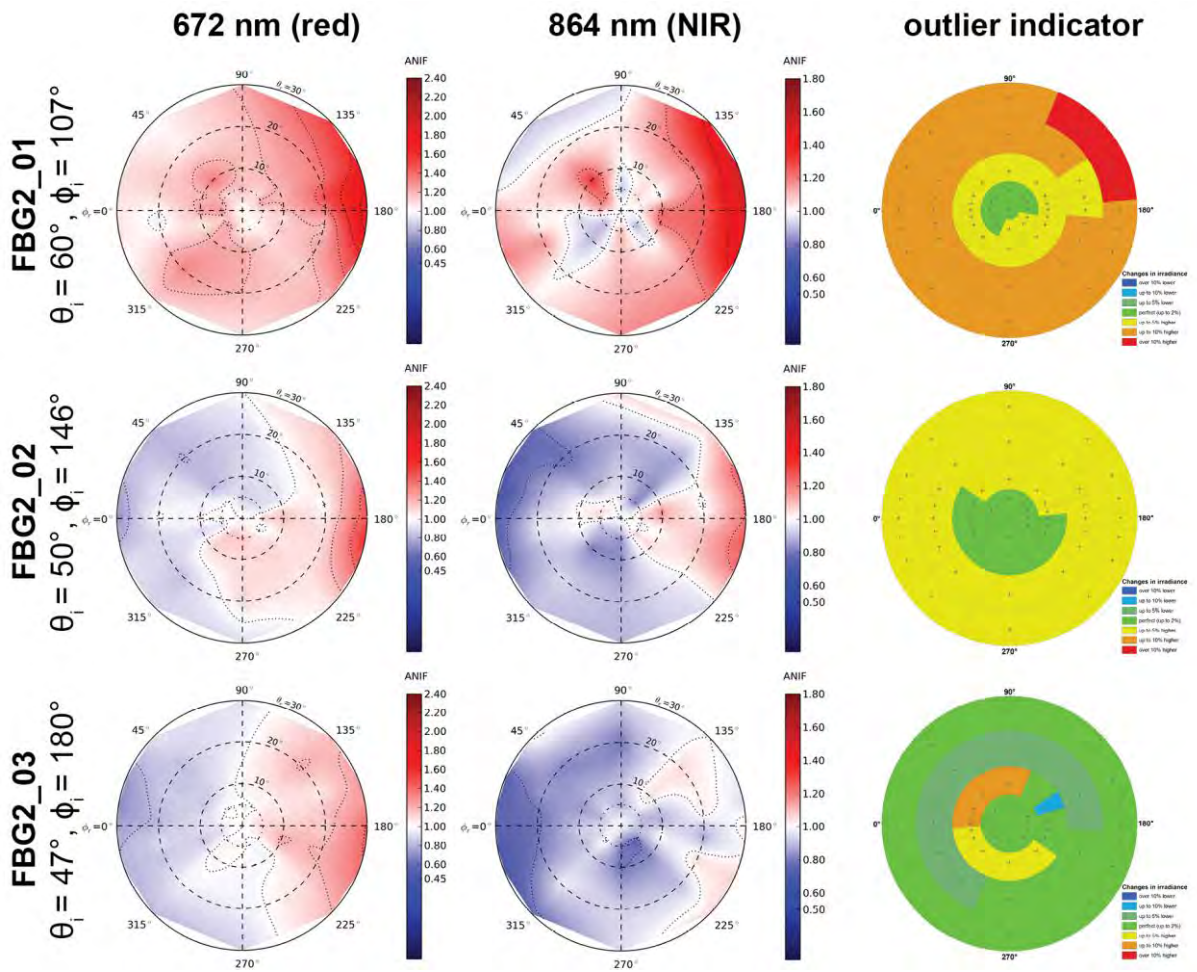


Figure C.2-13: ANIF visualization at 672 nm and 864 nm of the FBG2 site.

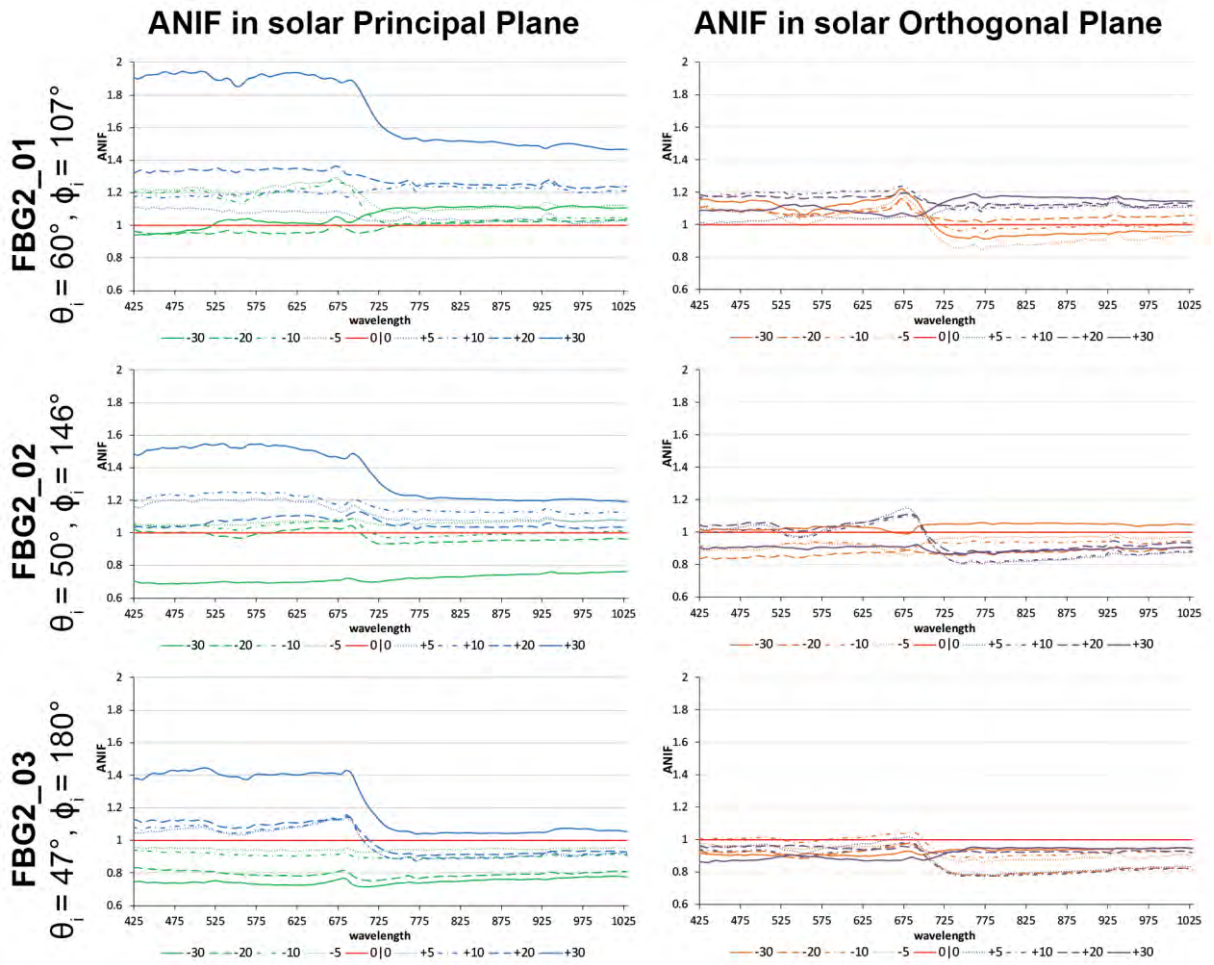


Figure C.2-14: ANIF visualization in principal & orthogonal plane of the FBG2 site.

VIII ANIX Visualization

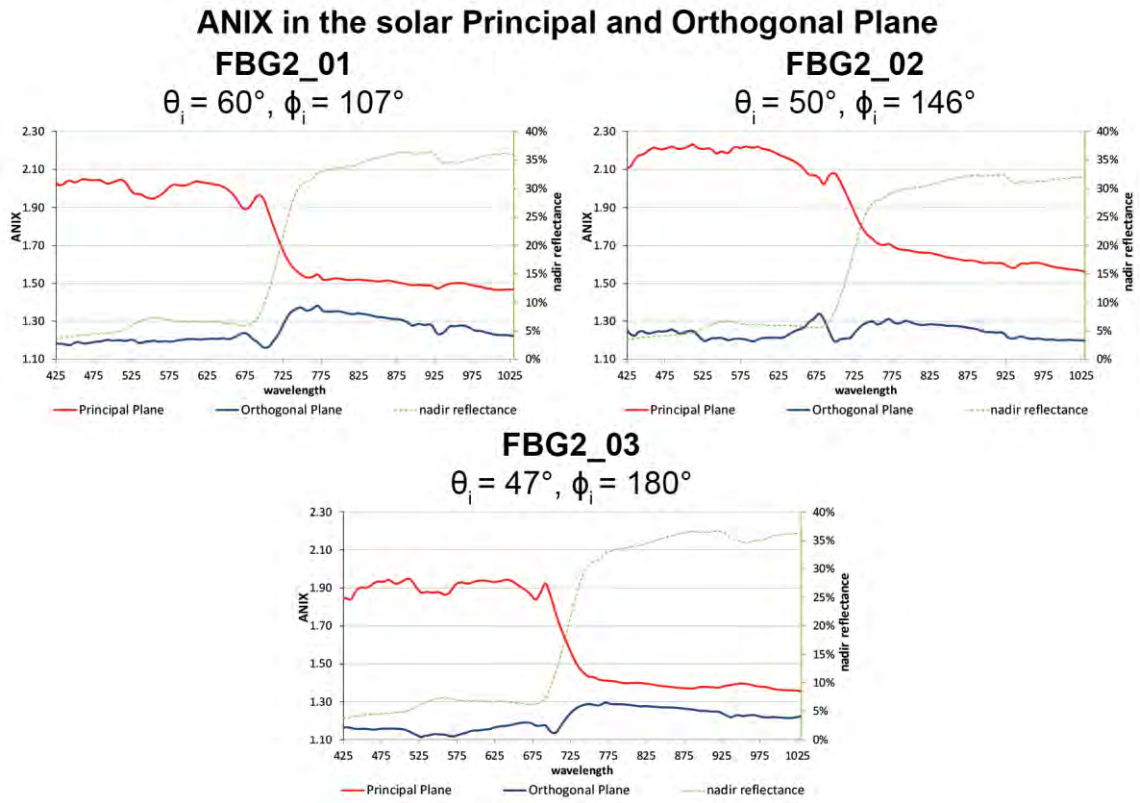


Figure C.2-15: Comparison of the ANIX in the solar principal and orthogonal plane with the nadir reflectance of the FBG2 site at different sun zenith angles.

IX NDVI and Relative Absorption Depth Visualization

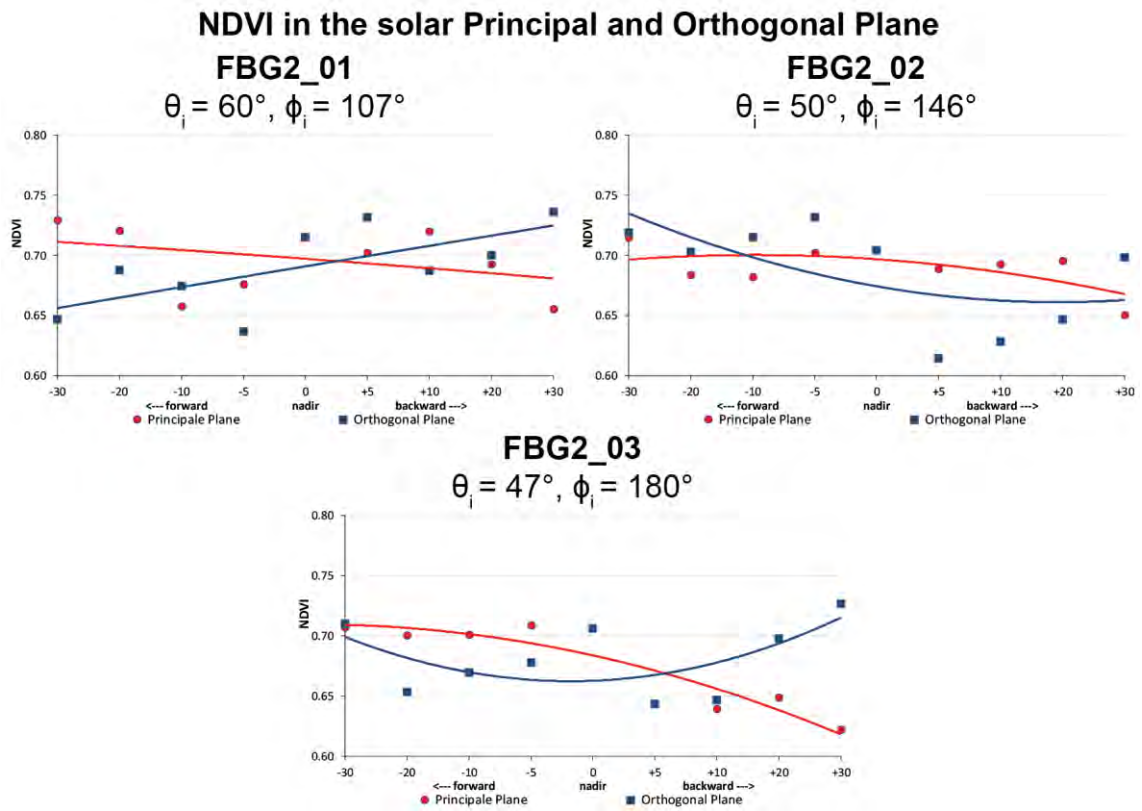


Figure C.2-16: Comparison of the NDVI in the solar principal and orthogonal plane of the FBG2 site at different sun zenith angles.

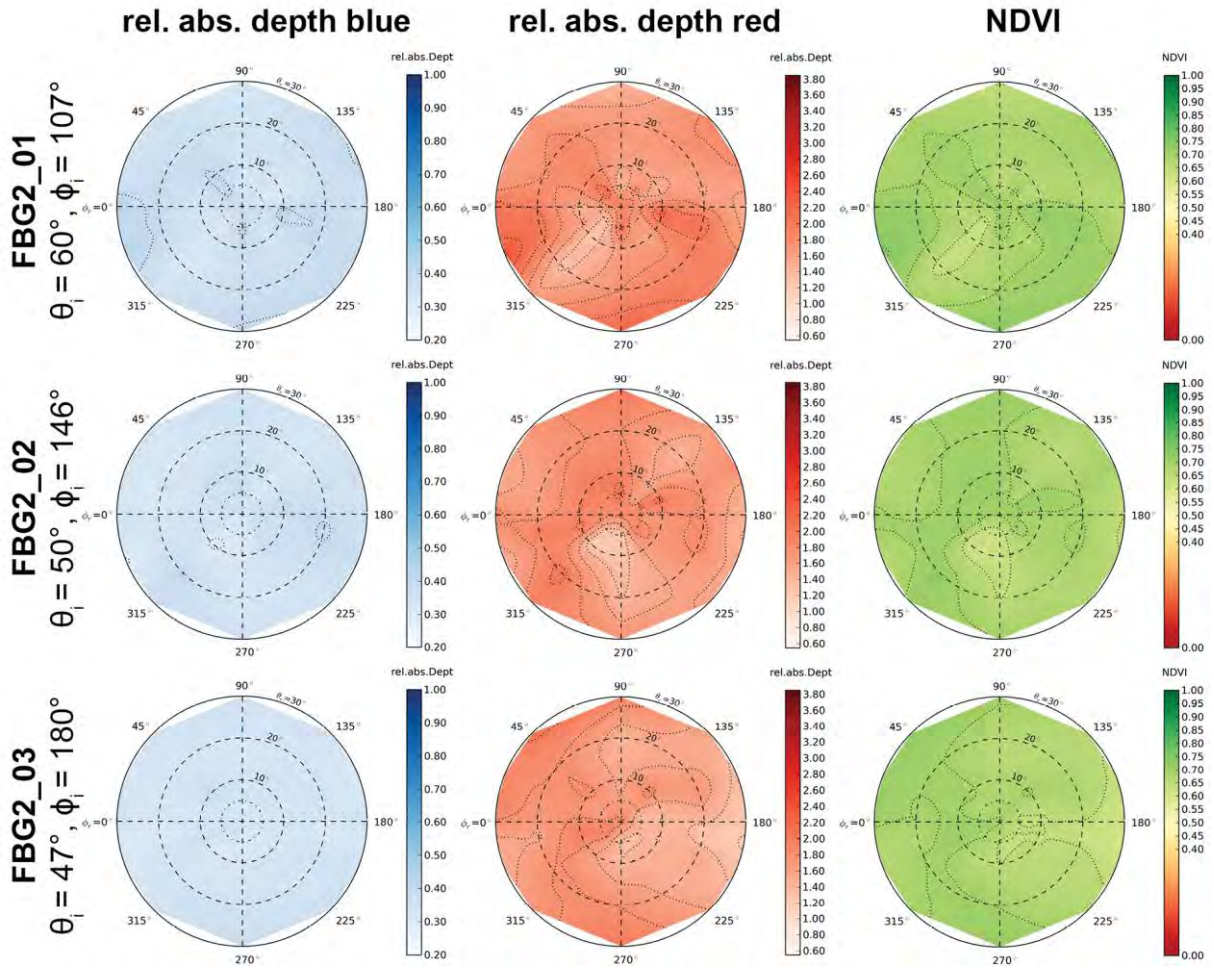


Figure C.2-17: Visualization of relative absorption depth & NDVI of the FBG2 site.

X NDVI Comparison of Different Sensors

Table C.2-5: Center wavelengths and band widths of the broadband and narrowband NDVIs, based on the spectral response curves of the AVHRR, MODIS and EnMAP sensors.

| NDVI | Sensor | Sensor band | Center wavelength (nm) | band width (nm) |
|---|---------|------------------------------|------------------------|-----------------|
| NDVI_{AVHRR} [broadband] | AVHRR/3 | red: band 1 NIR: band 2 | 630 865 | 100 275 |
| NDVI_{MODIS} [broadband] | MODIS | red: band 1 NIR: band 2 | 645 859 | 50 35 |
| NDVI_{EnMAP} [narrowband] | EnMAP | red: band 47 NIR: band 73 | 672 864 | 6.5 8 |

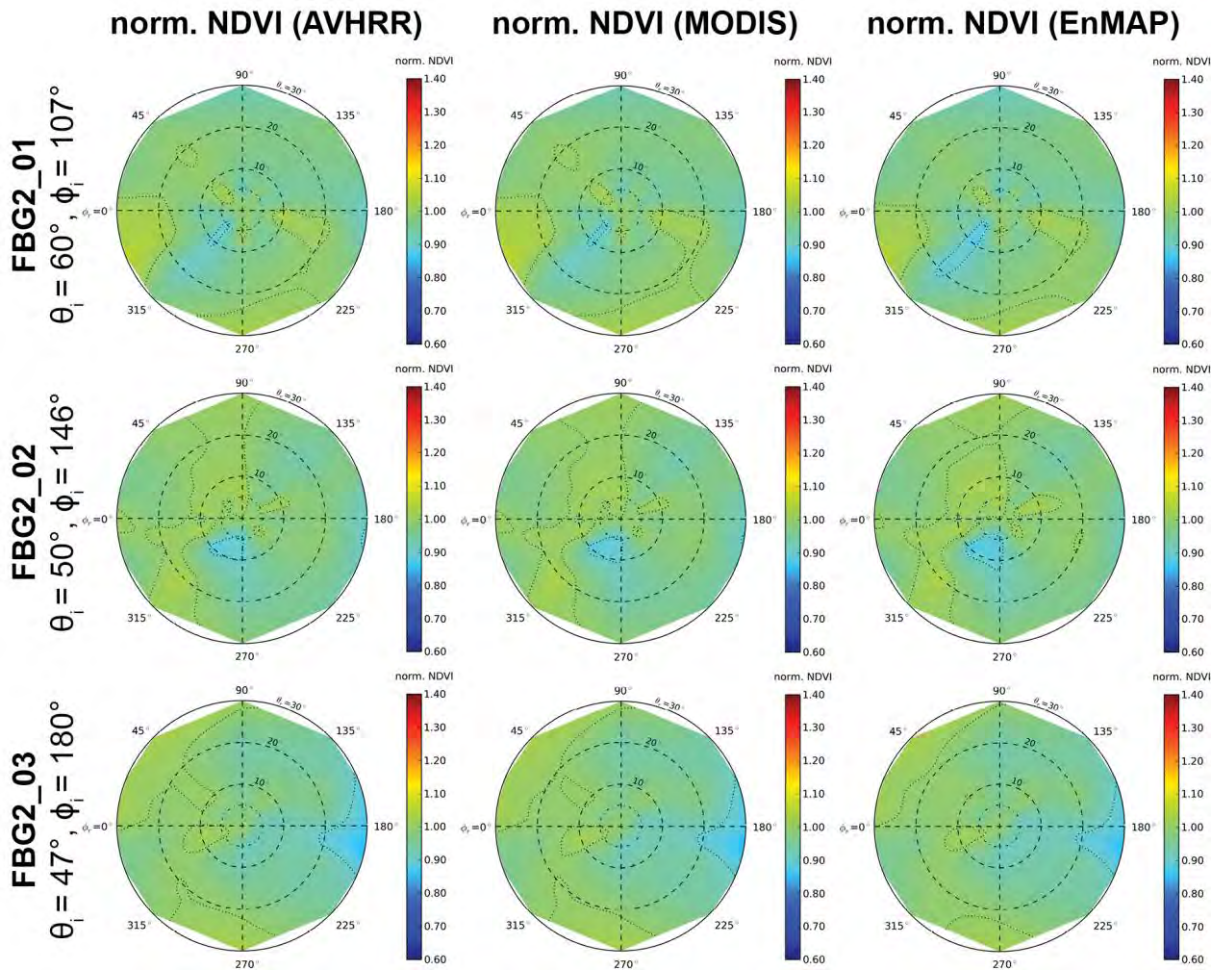


Figure C.2-18: Comparison of AVHRR, MODIS & EnMAP NDVI of the FBG2 site.